VESIENTUTKIMUSLAITOKSEN JULKAISUJA
PUBLICATIONS OF THE WATER RESEARCH INSTITUTE

60

John Forsius: Computing unsteady flow and tracer movement in a river
Tiivistelmä: Muuttuvan jokivirtauksen ja merkkiaineen kulkeutumisen laskeminen 3

Risto Kuittinen & Yrjö Sucksdorff: Determination of water depth using aerial photography
Tiivistelmä: Ilmakuvien käyttö vesistöjen syvyyssuhteiden määrittämisessä 22

Markku Puupponen: Measurement of flow rates at Finnish hydroelectric power stations
Tiivistelmä: Vesivoimalaitosten virtaaman mittaukset Suomessa 35

VESIHALLITUS—NATIONAL BOARD OF WATERS, FINLAND
Helsinki 1984

Tekijät ovat vastuussa julkaisun sisällöstä, eikä siihen voida vedota vesihallituksen virallisena kannanottona.

The authors are responsible for the contents of the publication. It may not be referred to as the official view or policy of the National Board of Waters.

ISBN 951-46-8842-2
ISSN 0355-0982

Helsinki 1985. Valtion painatuskeskus

COMPUTING UNSTEADY FLOW AND TRACER MOVEMENT IN A RIVER

John Forsius

FORSIUS, J. 1984. Computing unsteady flow and tracer movement in a river. Publications of the Water Research Institute, National Board of Waters, Finland, No. 60.

Two mathematical models are presented here. The USTFLO model simulates unsteady flow in a river and it is especially designed to simulate the discharge released from hydro-power plants. The DISPER model simulates the convection, dispersion and decay of a tracer or a pollutant in a river with unsteady flow. Both models were applied to the Nurmonjoki River. Water levels were quite accurately simulated with the USTFLO model. The DISPER model simulated the propagation time of the peak concentration of a tracer (Rhodamine) quite accurately, while peak concentration values and concentration distributions were simulated less accurately. This was mainly due to adsorption of the tracer on vegetation, which could not be taken into account in the simulation. However, it was concluded that the method of calculation used in the DISPER model is correct, and quite efficient. As a general conclusion both models were considered valuable especially in highly unsteady flow situations, due to the favourable numerical properties of the finite difference schemes used.

Index words: Unsteady flow model, transport of pollutants, convection-dispersion model, Preissmann scheme, Holly-Preissmann method, USTFLO model, DISPER model, Nurmonjoki River.

1. INTRODUCTION

Mathematical modeling of water flow has become widely used tool in river engineering. The reason is its remarkable success in dealing with a variety of flow situations in quite complex situations, where traditional analytical methods fail and hydraulic scale models become too costly. The simulation of river flow is based on the formulation and solution of equations expressing fundamental hydraulic principles; the simulation is, thus, physically sound. Efficient computers enable the use of large models, as the limits of core memory and processing time, imposed by the computer hardware, are pushed further away. Mathematical modeling is attractive from the economical point of view. The effect of different construction alternatives, different regulation schemes for hydro-power plants, etc., can easily be studied once the model is set up and calibrated.

Some users of mathematical models prefer to write the computer program themselves. Then they know exactly how the model is constructed,

and later modifications of the model are easy to make. To use an already existing model, developed by someone else, saves the user's time at the computer terminal; but usually the model still requires some sort of modification before it can be applied to a particular case. Whatever the case, the user should spend enough time to check the equations and the scheme used in the model, so that he knows what it is doing. This may seem as a superfluous remark, but too often models are used as black boxes, after the user has asserted that the model works technically. It should not be so. All models simulating water flow differ from each other in some respect, e.g. in the equations or the numerical scheme used or in the treatment of some terms in the equations. In a given situation one model, or scheme, is more suitable than another, and the user should be aware of this.

In this article two mathematical models related to the flow in rivers are presented. The first model to be described, USTFLO, simulates the unsteady flow of a river. It is especially designed to simulate the following:

— the propagation of flood waves through reservoirs and along rivers
— the discharge released from hydro-power plants
— the propagation of storm-induced floods in estuaries.

The model can be applied to a river with several dams or power plants in a row and to a tree-like branching river system. The model can be used only in subcritical flow situations, and points where supercritical flow occurs, e.g. weirs and bottom dams, have to be treated as boundary points.

The second model, DISPER, simulates the transport of a pollutant in a river with unsteady flow. It is designed to be used together with the USTFLO model, though it can be used quite independently. It can, of course, also be used in steady state conditions. The model calculates the convection, dispersion and first order decay of a pollutant. The most attractive feature of this model is the small numerical diffusion induced by the difference scheme, and thus it is accurate also in highly unsteady situations. The DISPER model can be used to determine the dilution and propagation time of a pollutant accidentally released upstream a drinking water intake, for example. Thus it would be possible to predict when the pollutant concentration level has increased so much that the water intake has to be shut down. If the discharge of the river is regulated by a hydro-power plant, the dilution can be increased by increasing the discharge. The DISPER model could be used to predict the effect of such a measure.

Both the unsteady flow model and the convection — dispersion model solve the governing equations with finite difference methods. The models have been constructed and operated by the Hydrological Office of the National Board of Waters, starting from the year 1981. Attention has been paid to making the models flexible and suitable for industrial use in a wide range of problems. The theory behind the models and the solution technique used in the models are proposed mainly by Cunge et al. (1980), as well as are some of the practical advice and suggestions to improve the models that appear in the text. Furthermore, the problems of setting up these models are discussed, together with the need for input data and model calibration.

Finally, a case study is presented to illustrate the practical merits of the two models. From the experience gained with the models it can be concluded that the models are most useful in rivers with short-term regulation.

The purpose of this article is a twofold one. Firstly, it is hoped that the reader, as a potential user of the models or as a user of model results, gets a good idea of the applicability of the two models, and of their limitations and constraints. The aim is to give information on which the reader will be able to judge the reliability of these models in a particular situation. Secondly, this article serves as a brief documentation, or manual, of the models. Therefore, the description of some procedures carried out within the model is quite detailed.

The worst thing that can happen to any mathematical model is that it is applied to a situation for which it is not intended. Then the obtained, obviously false, results will discourage from all further use of the model, and the credibility of mathematical modeling has received another blow.

2. THE USTFLO UNSTEADY FLOW MODEL

2.1 Equations

The model solves the full de Saint Venant equations numerically. The equations have for practical applications the following form:

$$b_{st}\frac{\delta y}{\delta t}+\frac{\delta Q}{\delta x}=q \qquad (1)$$

$$\frac{\delta Q}{\delta t} + \frac{\delta}{\delta x}\frac{(\beta Q^2)}{A} + gA\frac{\delta y}{\delta x} + gAS_f = 0 \qquad (2)$$

y = water surface elevation above datum
b_{st} = storage width
t = time
Q = discharge
x = longitudinal space co-ordinate in horizontal plane
q = lateral inflow
A = cross sectional area
g = acceleration due to gravity
S_f = friction slope
β = coefficient of non-uniform velocity distribution

Eq. (1) represents the conservation of mass and Eq. (2) the conservation of momentum. Eq. (2) is often called the dynamic equation.

The original de Saint Venant equations are based on the following assumptions:

(i) The flow is one-dimensional, i.e. the velocity is uniformly distributed in the cross sections, and the water level across the section is horizontal.
(ii) Vertical accelerations are negligible, and the pressure is hydrostatic.
(iii) The effects of turbulence and friction can be accounted for by resistance laws applicable to steady state flow.
(iv) The average channel bed slope is small so that the cosine of the angle it makes with the horizontal can be approximated to unity.

In natural water courses the cross sections are very irregular, and the velocity is not uniformly distributed in the cross section. Hence the original de Saint Venant equations have been modified by using the "storage width" concept in Eq. (2) instead of channel width; a velocity distribution factor β has also been introduced. The storage width has been introduced to handle a situation with overbank flow. When the river is flooding, almost all the momentum is conveyed in the main channel, and the overbank areas act only as storage areas for the water. Thus the effective, or live, cross sectional area used in the second term of Eq. (2) is less than the total cross section, see Fig. 1.

If the velocity distribution coefficient β is used, the need for defining a somewhat arbitrary live cross sectional area disappears. The value of β can be computed from Eq. (3):

$$\beta = \frac{\int_0^b u_z^2 h_z dz}{\bar{u}^2 A} \qquad (3)$$

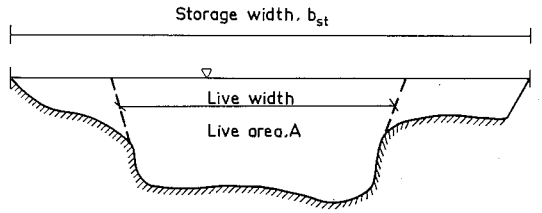

Fig. 1. Storage width and live area of a channel cross section.

where
u_z = local depth averaged velocity at position z in cross section
h_z = local depth at position z in cross section
$\bar{u}$ = mean cross sectional velocity

It is seen that the computation of β involves some effort and the calculation should, in principle, be based on measurements of flow velocity in the river. In practice, however, such measurements are hardly available, so β has to be computed on the base of assumptions of bed roughness (Cunge et al. 1980, p. 23). If no overbank flow occurs, there is no need for distinguishing between storage and live areas, and in this case the computed values of β would be very close to unity. In the USTFLO model the more arbitrary method of storage width and live area is used, because it is much simpler and requires less preparation of input data. However, in the computer program the possibility of using the β approach has been preserved, though a subroutine to determine the value of $\beta = \beta(y)$ has to be developed. In the present state the program uses a constant value of β, and it is recommended that its value should be in the range 1.0—1.1.

In the USTFLO model the resistance term S_f is calculated using the Manning approach:

$$S_f = Q^2/K^2 = Q^2/(M^2A^2R^{4/3}) \qquad (4)$$

K = conveyance
M = Manning number
$R = A/P$ = hydraulic radius
P = wetted perimeter of cross section.

The live area and live wetted perimeter of the cross section is used, and M is assumed to be constant. The most correct way to calculate the friction slope would be to divide each cross section into vertical slices and to use the total conveyance concept (Cunge et al. 1980, p. 22)

$$K = \sum_i K_i \qquad (5)$$

$K_i = M_i h_i^{5/3} \cdot b_i$
i = slice number
h_i = mean depth of slice
b_i = slice width.

The conveyance can then be expressed as a function of water stage, and it is more accurate to extrapolate conveyance values as such than the individual variables appearing in Eq. (4). Especially so in the case of overbank flow. It presents no problems to modify the USTFLO model to use the total conveyance concept, but this means additional work in the preparation of input data, and the difference between the two methods is small when there is no overbank flow.

2.2 Treatment of ice-covered rivers

The model can be applied to ice-covered rivers, if one can assume that there are no elastic effects arising from the ice cover and that the flow is not pressurized. This means that the ice cover is floating freely on top of the water, adding only weight to the vertical water column. This behavior can be expected in wide rivers, and an example of an application to an ice-covered river is given in Forsius (1984).

In the ice-covered case the cross section area, wetted perimeter and storage width is taken at a water level corresponding to the lower edge of the ice cover. A certain fraction of the width is added to the wetted perimeter values, to account for the additional friction caused by the ice cover. This fraction has to be given as input data.

The ice cover is assumed to be of constant thickness in each branch.

2.3 Solution technique

The equations (1) and (2) are solved by finite difference methods. The river is discretized into a finite number of gridpoints (cross sections) and the values of the state variables, stage and discharge, are calculated at discrete time intervals, whereby the approximate solution of the continous flow equations (1) and (2) is obtained. How close to the true solution one gets depends in general on how the discretization of the individual terms in the equations is done, it depends on the distance step and on the time step used in the discretization, and it depends on the combination of these things. The USTFLO model uses Verwey's variant of the Preissmann discretization scheme (Cunge et al. 1980):

$$(b_{st})^{n+\Theta}_{j+1/2}\left(\frac{y^{n+1}_j - y^n_j}{2\Delta t} + \frac{y^{n+1}_{j+1} - y^n_{j+1}}{2\Delta t}\right) + \Theta\frac{Q^{n+1}_{j+1} - Q^{n+1}_j}{\Delta x} + (1-\Theta)\frac{Q^n_{j+1} - Q^n_j}{\Delta x} - q^{n+\Theta}_{j+1/2} = 0 \quad (6)$$

$$\frac{1}{2}\frac{Q^{n+1}_j - Q^n_j}{\Delta t} + \frac{1}{2}\frac{Q^{n+1}_{j+1} - Q^n_{j+1}}{\Delta t} + \left(\frac{Q^n_{j+1}\,Q^{n+1}_{j+1}}{A^{n+1/2}_{j+1}} - \frac{Q^n_j\,Q^{n+1}_j}{A^{n+1/2}_j}\right)\frac{\beta}{\Delta x} + g A^{n+\Theta}_{j+1/2}\left(\Theta\frac{y^{n+1}_{j+1} - y^{n+1}_j}{\Delta x} + (1-\Theta)\frac{y^n_{j+1} - y^n_j}{\Delta x}\right) + \frac{1}{2} g A^{n+1/2}_{j+1/2}\left(\frac{|Q^n_j|\,Q^{n+1}_j}{(K^2)^{n+1/2}_j} + \frac{|Q^n_{j+1}|\,Q^{n+1}_{j+1}}{(K^2)^{n+1/2}_{j+1}}\right) = 0 \quad (7)$$

j = computational point index
n = computational time step index
Δx = distance between points j and $j+1$
Δt = time between n and $n+1$
Θ = weighting factor; $\Theta \geq 0.5$.

The scheme is stable for $\Theta \geq 0.5$.

The scheme is also called a box scheme, because it uses information from four points in the $x - t$ domain, namely from the points (j, n), (j + 1, n), (j, n + 1) and (j + 1, n + 1). The choice of this type of scheme is favored by the following:

(i) If $\Theta = 0.5$, the approximation of the derivatives is of second order; this means that if e.g. Δx is divided by two (= the distance between computational gridpoints is halved), the error in the approximation of the space derivatives is reduced by a factor of four. A varying Δx does not affect the order of approximation. Not all existing schemes have this feature.

(ii) By setting $\Theta > 0.5$ the stability of the scheme increases and makes it possible to simulate steep fronts appearing e.g. in supply channels of hydro-power plants. The accuracy of the scheme, however, decreases and is no longer of second order.

(iii) The scheme is implicit and imposes no restrictions on the length of the time step to be used, contrary to explicit schemes.

(iv) The scheme computes both the stage and discharge in the same gridpoint. Some widely

used schemes, e.g. the Abbott-Ionescu scheme (Abbott 1979), compute the stage and discharge in separate points, and this may create problems at boundaries or in junctions of channels. These difficulties are, thus, avoided with the current scheme.

2.4 Solution algorithm

Because the Preissmann scheme is implicite, it requires a certain solution algorithm. For a pair of adjacent points (j, j + 1) the equations (6) and (7) are written as

$$A1_j Q_j + B1_j y_j + C1_j Q_{j+1} + D1_j y_{j+1} = E1_j \qquad (8)$$

$$A2_j Q_j + B2_j y_j + C2_j Q_{j+1} + D2 y_{j+1} = E2_j \qquad (9)$$

The superscript n + 1 is left out from the Q and y variables, for the sake of clarity. The expressions for the coefficient A1, B1 ... D2, E2 are obtained by collecting terms from equations (6) and (7).They are given in appendix 2. For N number of points (cross sections), N-1 pairs of such equations, or a total of 2N-2 equations can be written to solve 2N unknowns (Q and y) at each time level.

As two boundary conditions must be supplied, one actually has 2N equations, and the system can be solved. The resulting matrix is banded and five-diagonal. This matrix is solved with the double sweep method described e.g. by Liggett and Cunge (1975, p. 149 ff.) A short description is given here, because it helps to understand how the boundary conditions are formulated in the computer program.

Using the relations

$$Q_j = F_j y_j + G_j \qquad (10)$$

$$y_j = H_j Q_{j+1} + I_j y_{j+1} + J_j \qquad (11)$$

and inserting these in equation (9) one obtains:

$$H_j = -C1_j/(B1_j + A1_j F_j) \qquad (12)$$

$$I_j = -D1_j/(B1_j + A1_j F_j) \qquad (13)$$

$$J_j = (E1_j - A1_j G_j)/(B1_j + A1_j F_j) \qquad (14)$$

By inserting equations (11) and (12) in equation (10) one obtains, after some manipulation, the recurrence relations

$$F_{j+1} = -(\alpha^* I_j + D2_j)/(\alpha^* H_j + C2_j) \qquad (15)$$

$$G_{j+1} = (E2_j - A2_j G_j - \alpha^* J_j)/(\alpha^* H_j + C2_j) \qquad (16)$$

$$\alpha^* = A2_j F_j + B2_j$$

In the first sweep from point j = 2 to point j = jj (jj = last gridpoint) the values of F_j and G_j are computed. This sweep is initialized by giving values to F_1 and G_1, obtained from the boundary condition in the first gridpoint. How these values are obtained is explained in section 2.5.

The return sweep from point jj to point j = 2 is initiated by applying the boundary condition in point jj, from which Q_{jj} and y_{jj} can be computed (see section 2.5.). Then the equations (10) and (11) are used to compute the Q_j and y_j values in the remaining points. Because the difference scheme is non-linear, i.e. contains coefficients at time levels higher than n, at least two iterations for the solution at each time level have to be performed. During the first iteration the solution at time level n + 1 is defined using the coefficients at time level n. In the second iteration the solution is improved by using for the coefficients average values at time level n + 1/2 or weighted values at time level n + Θ defined with the solution of the first iteration. In the USTFLO model the user can choose the number of iterations to be performed, but experience has shown that using three or more iterations does not improve the results obtained with two iterations only.

2.5 Boundary conditions

The USTFLO model requires that boundary conditions are supplied both at the upstream and at the downstream end of each river reach. The boundary conditions are either called external or internal boundary conditions. External boundary conditions that can be applied are:

- the discharge as a tabulated function of time
- the water level as a tabulated function of time
- the discharge given as a tabulated function of water level (a Q − y relationship).

The two first-mentioned conditions can be applied both to the upstream and downstream end, the last one to the downstream end only.

Internal boundary conditions are applied in internal computational points:

- in the junction of two rivers
- in points where there is additional head loss due to a constriction, e.g. a bridge opening.

To start the first sweep in the double sweep procedure the F_1 and G_1 values have to be

initialized. From Equation (11) it is seen that:
1) when discharge is given $F_1 = 0$, $G_1 = Q_1^{n+1}$.
2) when water level is given

$$y_1^{n+1} = \frac{Q_1}{F_1} - \frac{G_1}{F_1} \tag{17}$$

In the USTFLO model $F_1 = 5 \cdot 10^4$ and $G_1 = -F_1 y_1^{n+1}$ in the second case, and then the first term of the right hand side of Equation(17) will go to almost zero. As an example, if the discharge is 500 $m^3 s^{-1}$ an error of $500/5 \cdot 10^4 = 10^{-2}$ m in water level at the boundary is made; but this error is usually negligible in practical situations. However, the user should be aware of the error thus introduced.

At the downstream end the boundary condition is expressed with a general relation

$$y_{jj} = (\gamma_{jj} - \alpha_{jj} G_{jj})/(\beta_{jj} + \alpha_{jj} F_{jj}) \tag{18}$$

The values of α_{jj}, β_{jj} and γ_{jj} depend on the boundary condition according to the following:
1) Discharge is given: $\alpha_{jj} = 1$, $\beta_{jj} = 0$, $\gamma_{jj} = Q_{jj}^{n+1}$
2) Water level is given: $\alpha_{jj} = 0$, $\beta_{jj} = 1$, $\gamma_{jj} = y_{jj}^{n+1}$
3) A Q–y relationship is used (see Fig. 2 for notation):

$$\alpha_{jj} = 1, \beta_{jj} = -\frac{dQ}{dy}, \gamma_{jj} = Q_k - \frac{dQ}{dy} y_k$$

This is equivalent to

$$Q_{jj}^{n+1} = Q_k + \frac{dQ}{dy}(y_{jj}^{n+1} - y_k) \tag{19}$$

If there are several power plants or weirs along the same river, the stretches between these regulating structures are treated as separate channels where the lower boundary of the first stretch is the regulating structure, the upper boundary of the second stretch is the discharge computed at the first structure, etc. In this way a series of e.g. power plants can be modeled in one computer run.

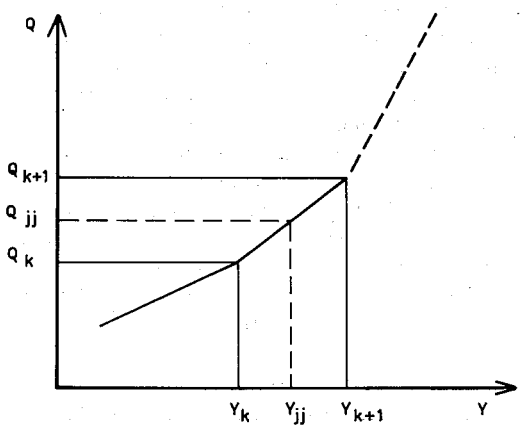

Fig. 2. Discretization of a Q – y relationship at the downstream boundary.

Internal boundary conditions that can be used in the USTFLO model are:
1) Water level compatibility in junctions. This assumption is correct as long as the velocity head is small.
2) The additional head loss Δy due to a constriction is computed with

$$\Delta y = \mu \frac{(V_1 - V_2)^2}{2g}$$

V_1, V_2 = flow velocity in sections 1 and 2, respectively
μ = head loss coefficient.

The value of μ can be obtained using a procedure described by Chow (1959, p. 476 ff).

2.6 Input data files

The data requirements for the unsteady flow model are distributed in four different files:
1) river geometry data file
2) boundary data file
3) initial condition data file
4) parameter data file

The river geometry data consist of the area, wetted perimeter and storage width of each cross section, tabulated against at most 5 water levels. Also the distance from the starting point is given for each cross section. All units are metric ones. If the computed water level, during computation, is outside the tabulated range, the corresponding geometrical data are obtained by linear extrapolation.

In the boundary data file one has to define the type of the boundary condition to be used; the data are given as tabulated functions. If there are several reaches or branches in the river system, boundary conditions have to be specified for each reach separately. The time scale used in the tabulation, hours, minutes or seconds, has also to be specified.

The initial data file consists of the values of water level and discharge for each gridpoint needed to start the computation at the first time level. Usually these data are not known a priori, and the model has to run for some time to adjust itself to e.g. a correct steady state condition. But it has

turned out that the model can go unstable after only a few time steps, if the given initial conditions are very far from the true values. In these unstable cases either the river bed went dry or supercritical flow occurred. To ensure that the computation gets started there are four options to give the initial data:

1) The water level and discharge is given for each gridpoint separately.
2) Only one water level — discharge pair is given; the model assumes these values for all gridpoints.
3) Two water level — discharge pairs are given for each branch or reach; the model assumes that the first pair is the upstream point and the second pair the downstream point. The in-between values are obtained by linear interpolation.
4) The model assumes that the discharge is zero and the initial water level in each gridpoint is the highest tabulated water level for that cross section appearing in the river geometry file.

Errors in the supplied initial data are quickly washed out, as the computation goes on. If a steady state situation is the right initial situation, the process can be speeded up by using the TSTART and WIDTHCON variables in the parameter file. The storage width is decreased by a factor equal to WIDTHCON for a time TSTART before the actual simulation begins.

The parameter data file consists of data relating to the river and of data relating to the computational procedure and the output of results.
Parameters relating to the river are:

— Manning number
— lateral inflow
— ice thickness
— coefficients of velocity distribution and of singular head loss
— information on how the different branches are connected to each other

Data for the computational procedure are

— time step
— weighting coefficient Θ
— number of iterations to be performed
— simulation time span
— the numbering of gridpoints
— the order in which the first sweeps in the branches are to be made
— the direction of the first sweep in each branch.

The solution algorithm demands that the computations are carried out in a definite order, and the principle to be followed will be explained in the case of a junction (Fig. 3). The first sweep is initiated at ① and carried along channel A to point 11. Then a sweep is made along channel B from ② to 21. Then the water level compatibility criterion is assumed by the model, i.e.

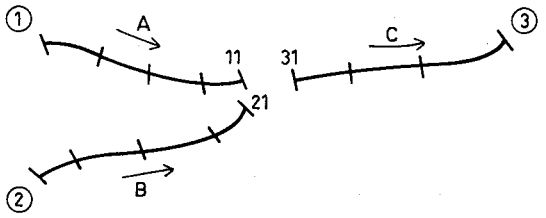

Fig. 3. Solution algorithm for junctions in the USTFLO model (after Cunge et.al., 1980).

$$F_{11} + F_{21} = F_{31}$$
$$G_{11} + G_{21} = G_{31}$$

and the sweep along channel C is continued. The backsweeps are then performed in the opposite order. The water flow direction relative to the sweep direction is of no importance, but the positive x direction is always in the direction of the first sweep.

Instructions concerning the output are:

— points from which output is wanted
— the desired interval (in terms of time step) for the output.

The output consists of simulation time, computed stage and computed discharge.

2.7 Discretizing the natural river

When the natural river is modeled by choosing certain discrete points where the river geometry is known, it is important that these points are representative for that particular stretch of the river. The number of gridpoints to be used and the distance Δx between them depends on the river. Finnish rivers are generally quite irregular, and a Δx in the order of 100...500 m is usually required. Sudden constrictions have to be modeled with a very short Δx, and the head loss coefficient might have to be defined as well, to account for a singular head loss. Experience has also shown that a shorter Δx has to be used near regulating hydro-power stations, to decrease numerical diffusion. The choice of distance step and time step is also influenced by the resolution one wishes to have.

The discretization has to begin from a point where there exists a well-defined boundary condition, usually a reservoir, whose water level is

known, or a power plant whose discharge is known. Likewise, in the last point of the model the boundary conditions must be known.

No difficulties with memory overflow or unacceptable CPU-time requirements have turned up in experiments with up to 200 gridpoints and more than 1000 time steps on an ECLIPSE MV/6000 computer.

2.8 Difficulties encountered in applications of the USTFLO model

During the several applications of the USTFLO model to Finnish water courses some difficulties have turned up. The problem with unnatural initial conditions has already been mentioned. Problems have been encountered in rivers with heavy daily regulation, because supercritical flow has appeared in critical cross sections during times of low discharge, with subsequent instability of the computation. The remedy has usually been to lower the bottom artificially in that cross section.

In one application an artificial boundary condition (a Q − y relation) was imposed at the critical cross section, but such a measure introduces an error in the final solution also when the flow is subcritical. Some experiments in which the bottom friction was increased artificially at low water levels to keep the water level above the critical level showed that numerical instability easily occurred.

3. THE DISPER CONVECTION-DISPERSION MODEL

3.1 Equations

The model solves the convection and dispersion of a tracer in the one-dimensional case by the equation:

$$\frac{\delta}{\delta t}(AC) + \frac{\delta}{\delta x}(AUC) - \frac{\delta}{\delta x}\left(AK\frac{\delta C}{\delta x}\right) = \frac{q}{A}(C_L - C) - kC \qquad (20)$$

C, U = the cross-sectional average concentrations and velocities, respectively
K = longitudinal mixing coefficient
C_L = load from a source of discharge
k = linear decay coefficient.

The longitudinal mixing coefficient includes the effects of molecular diffusion, turbulent diffusion and the difference in convection velocities within a cross section, also called dispersion. Usually the dispersion is the dominant factor in the mixing process, and K is therefore sometimes called the dispersion coefficient.

The solution of Eq. (20) is carried out in three steps. In the first step the pure convection of the tracer is calculated with Eq. (21):

$$\frac{\delta}{\delta t}(AC) + \frac{\delta}{\delta x}(AUC) = 0 \qquad (21)$$

In the second step the dispersion is calculated with Eq. (22):

$$A\frac{\delta C}{\delta t} = \frac{\delta}{\delta x}\left(AK\frac{\delta C}{\delta x}\right) \qquad (22)$$

In the final step the dilution and decay are computed with Eq. (23):

$$\frac{\delta C}{\delta t} = -\frac{q}{A}(C_L - C) - kC \qquad (23)$$

The equations (21)–(23) are solved explicitly with finite difference methods.

There are three options to select the value of the dispersion coefficient K:

1) K is a constant
2) K is a function of flow velocity and river geometry:

$$K = aUA/B \qquad (24)$$

B = surface width of cross section
a = a coefficient (Hess and White 1975)

3) K varies according to a procedure outlined by Liu (1977) with the final result:
$K = b\,Q^2\,U_*^{0.5}/(U^{1.5}\,R^3)$
$U_* = (g\,R\,S)^{0.5}$ = friction velocity
S = slope of energy gradient
b = coefficient with value 0.18 according to Liu (1977)

Case 3) can be used only for steady state calculations. In the unsteady case U can become zero and hence the dispersion will be infinitely large.

3.2 Solution technique

The convection equation (21) is solved with the explicit method developed by Holly and Preiss-

mann (1977), called the "two-point fourth-order method". It is a method of characteristics, and not only the concentration values but also the concentration gradients are convected. In this way it is possible to construct a scheme of fourth order accuracy using only two computational points.

If the concentration is denoted C, the gradient $\delta C/\delta x$ denoted CX and the Courant number $U\,\Delta t/\Delta x$ denoted Cr, the convected concentration at time level $(n+1)$ is:

$$C_j^{n+1} = a_1 C_{j-1}^n + a_2 C_j^n + a_3 CX_{j-1}^n + a_4 CX_j^n = 0 \quad (25)$$

where

$a_1 = Cr^2\,(3 - 2\,Cr)$
$a_2 = 1 - a_1$
$a_3 = Cr^2(1 - Cr)\,(x_j - x_{j-1})$
$a_n = Cr\,(1 - Cr)^2\,(x_i - x_{j-1})$

The subscript j refers to the gridpoint number.

A similar expression is used for the convection of the concentration gradient CX:

$$CX_j^* = b_1\,C_{j-1}^n + b_2\,C_j^n + b_3\,CX_{j-1}^n + b_4\,CX_j^n \quad (26)$$

where

$b_1 = 6\,Cr\,(Cr - 1)/(x_j - x_{j-1})$
$b_2 = -b_1$
$b_3 = Cr\,(3\,Cr - 2)$
$b_4 = (Cr - 1)\,(3\,Cr - 1)$

To account for a non-uniform velocity between x_j and x_{j-1} Eq. (29) is used:

$$CX_j^{n+1} = CX_j^*(1 - \Delta t\,(U_j - U_{j-1}))/(x_j - x_{j-1}) \quad (27)$$

The value of U appearing in the definition of the Courant number Cr is obtained by using the average of the velocity in point j and the velocity resulting from a linear interpolation on the x axis between points j and $j-1$ with an argument $U_j\,\Delta t$.

The scheme is stable for $Cr \leq 1.0$. According to Holly and Preissmann (1977), it introduces very little numerical diffusion, even in cases where the Courant number considerably deviates from unity. This makes the scheme especially suitable in short term regulated rivers, where the flow velocity (and hence the Courant number) varies widely in time. Several other schemes introduce a numerical diffusion that can be larger than the actual physical diffusion (Cunge et al., 1980).

The diffusion equation (22) is solved with the explicit scheme of Chevereau and Preissmann (cf. Cunge et al. 1980), using the concentrations obtained after the convection calculation as initial values. The difference scheme is:

$$C_j^{n+1} = C_j^n - \left[\frac{\Delta t}{A_j(x_{j+1/2} - x_{j-1/2})}\right. A_{j-1/2}K_{j-1/2}\,\frac{C_j^n - C_{j-1}^n}{x_j - x_{j-1}} - \left. A_{j+1/2}K_{j+1/2}\,\frac{C_{j+1}^n - C_j^n}{x_{j+1} - x_j}\right] \quad (28)$$

The scheme is stable as long as

$$\frac{K\,\Delta t}{(x_{j+1} - x_j)\,(x_j - x_{j-1})} \geq 0.5$$

Finally the dilution and decay of the tracer are calculated with Eq. (29):

$$C_j^{n+1} = C_j^n - \frac{q_j}{A_j}(C_L - C)_j^n - k\,C_j^n \quad (29)$$

3.3 Boundary and initial conditions

The concentration values and the concentration gradient values in each point at the beginning of the computation are used as initial conditions for the convection equation (Eq. 21). The gradient values can be set to zero in most applications, without gross errors in the final result. As boundary conditions both the C and the CX values have to be supplied at the upstream end. In practice, the C values obtained as a function of time through field measurements are used as upstream boundary conditions, and the CX values can be approximated by:

$$CX_{j=1} = -\frac{1}{U}\left(\frac{\delta C}{\delta t}\right)_{j=1} \quad (30)$$

The boundary conditions required by the diffusion equation, Eq. (22), are supplied automatically by the model. At the upstream end the model uses the known (measured) C values in this point, and at the downstream boundary a condition of no diffusion is assumed. The initial conditions: the C values obtained with the convection equation.

In the dilution-decay equation, Eq. (23), the upstream boundary condition is the known variation of the concentration; the initial conditions: the C values computed with the diffusion equation. These values are also automatically supplied by the DISPER model.

3.4 Input data requirements

The input data are supplied by files for:
— river geometry data

— boundary data
— flow data
— parameter and organizational data.

As mentioned earlier, the DISPER model can use flow data generated by the USTFLO model and the same river geometry file. One must keep in mind, though, that the time step used in DISPER is restricted by the Courant number condition $Cr \leq 1$. This means that, if a short distance step is used at the flow modeling stage with the USTFLO model, a short time step has to be used in the DISPER model. The only way to increase the time step is to increase the distance step by discarding cross sections from the river geometry file, using subjective judgement. At the flow modeling stage this can be accounted for by generating output only for those gridpoints used in the DISPER simulation.

The boundary data are expressed as values of concentration and concentration gradient tabulated as functions of time. The lateral inflow is also tabulated in the same manner.

In the flow data file the discharge and water level in each gridpoint as a function of time has to be given. To use the output file from the USTFLO model is convenient.

The parameter file consists of data necessary for the execution of the program, and of values for the diffusion coefficient and time step.

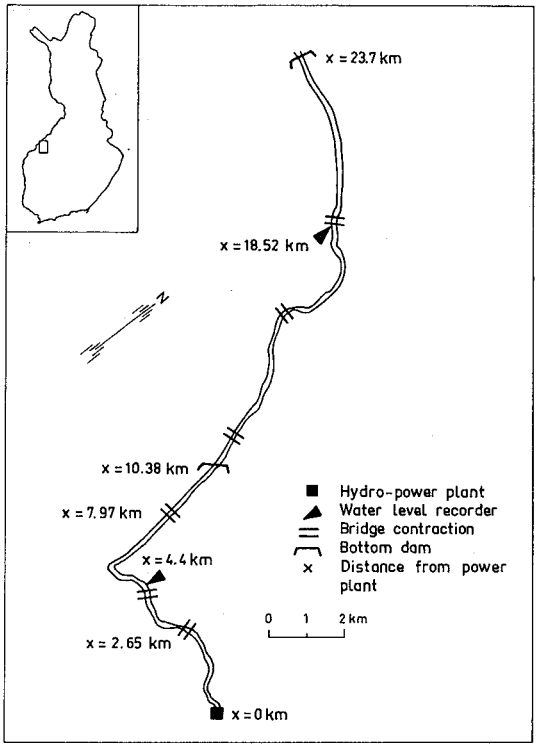

Fig. 4. The Nurmonjoki River.

4. MODEL APPLICATIONS

4.1 Unsteady flow in the Nurmonjoki River

The Nurmonjoki river is a small river, about 20 m wide and with a bottom slope of about 10^{-3}. Its discharge is controled by a hydro-power plant, and a 23.7 km long reach beginning at the power plant was simulated (Fig. 4).

This reach included two bottom dams, which were treated as boundary points. They served as overflow weirs in this particular application. Thus, the river stretch was treated as two separate reaches. The reported discharge from the power plant was used as upper boundary for the first reach, and the theoretical rating curve for the bottom dam 10.38 km downstream used as the downstream boundary condition. The computed discharge at this bottom dam was then used as the upper boundary for the second reach, and the (theoretical) rating curve for the second bottom dam used as the lower boundary. Three bridge constrictions were treated as internal boundary conditions, i.e. additional head losses were assumed in these points. The influence of the constrictions was minor, though, and could have been neglected without loss in accuracy.

The total reach was described with 43 measured cross sections, giving a mean Δx of 564 m. The time step used was 300 seconds. As initial conditions a horizontal surface was assumed, but the model was run for some time to wash out the initial conditions, before comparing computed and measured water levels. The model was calibrated by changing Manning number M until the computed water levels agreed with the measured ones 4.4 km and 18.52 km downstream the power plant. The agreement was determined by visual inspection, and best agreement was obtained with Manning numbers 25 $m^{1/3}\ s^{-1}$ for the upper stretch and 28 $m^{1/3}\ s^{-1}$ for the lower one, which are comparable with the text-book values, e.g. Henderson (1966). The result is shown in Fig. 5. As can be seen, the simulated and measured water levels agree quite well.

4.2 Tracer experiment in the Nurmonjoki River

The DISPER model was used to simulate the transport of a tracer, Rhodamine, during highly unsteady conditions in the Nurmonjoki River (Forsius et al. 1983). The tracer was injected immediately downstream the hydro power plant at a time when the turbines were operating at maximum capacity, thus ensuring initial mixing of the tracer. Concentration distributions (as a function of time) were measured with a through-flow fluorometer at four locations along the river, and the measured concentration distribution closest to the power plant was used as the upper boundary. The concentration gradient at the upper boundary was estimated with Eq. (30). The location of the measurement sites is indicated in Fig. 5. The mean discharge of the river was 1.7 m^3 s^{-1} during the field test (24th—27th August, 1982) but the main part of the total water volume was released in one-hour bursts three times a day. Hence the discharge variation was 0.1—12.5 m^3 s^{-1} at the power plant and 0.4—2.9 m^3 s^{-1} at x = 10380 m.

The USTFLO model was used to generate the water level and discharge in the different gridpoints for the whole period of the experiment. At first the original grid was used (mean Δx = 564 m), but this caused unacceptable numerical diffusion during the convection stage of simulation. Therefore the distance step was decreased by increasing the number of cross sections. The cross sectional characteristics (area, wetted perimeter, storage width) were obtained by linear interpolation of the original grid. The final mean Δx used was 103 m and the same grid was used both for the flow model and the convection-dispersion model. The use of the refined grid decreased the numerical diffusion, but a numerical diffusion was present still. For example, the peak concentration of the concentration distribution at the upper boundary will pass unaffected down the river, if a condition of no diffusion is assumed (K = 0 m^2 s^{-1}), but in this case it was reduced to 66 % of its original value at a point 8 km downstream. This numerical diffusion was, however, much less than the physical one, and was considered acceptable. It shows, though, that one always has to test models for numerical diffusion.

With a time step of 150 seconds the Courant number varied in the range 0.012—0.935 during the simulation. The dispersion coefficient K was calculated according to K = aUA/B (Eq. 24), and two different values for a were tested. With a = 10, K got a value 0.1—3.8 m^2 s^{-1}, and with a = 25 the diffusion coefficient was 0.2—9.4 m^2 s^{-1}. The results are shown in Fig. 6.

It can be seen that a fairly good correspondence is obtained at x = 4400 m when a = 10, but further downstream the better agreement is obtained with a = 25.

The shape of the concentration distribution curves differs from what one is accustomed to in steady flow situations. The reason is, of course, unsteady flow in the river. For example, the calculated sharp rise and decline of the concentration at x = 7970 m originate from the coincidence of peak concentration and peak flow velocity. The tracer cloud passes the observation point when the flow velocity is high and the concentration gradient large. Later, when both the flow velocity and the concentration gradient decrease, the curve flattens out. In this case the modeled shape of the distribution curve is sensitive to the arrival time of the tracer cloud. In other words, if the convection of the tracer cloud is computed incorrectly, the shape of the distribution curve will be severely distorted.

The amount of tracer recovered in the field at x = 10380 m was only 33 % of the original amount injected in the river, indicating losses due to adsorbtion of the tracer on vegetation, bottom gravel etc. Thus the model will compute higher maximum concentration values than the observed

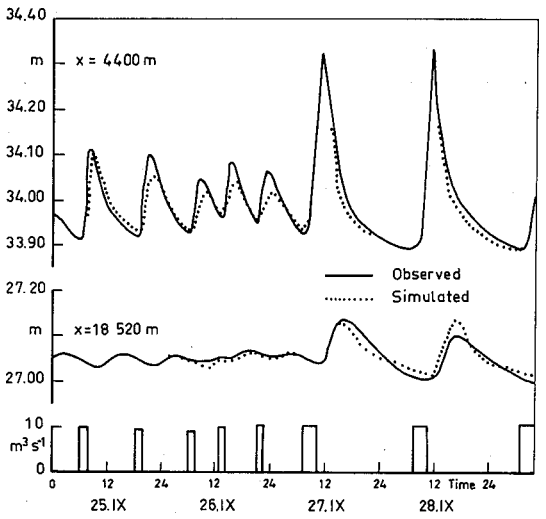

Fig. 5. Observed and simulated water levels in the Nurmonjoki River 4 400 m and 18 520 m downstream of the hydro-power plant, and the discharge of the power plant.

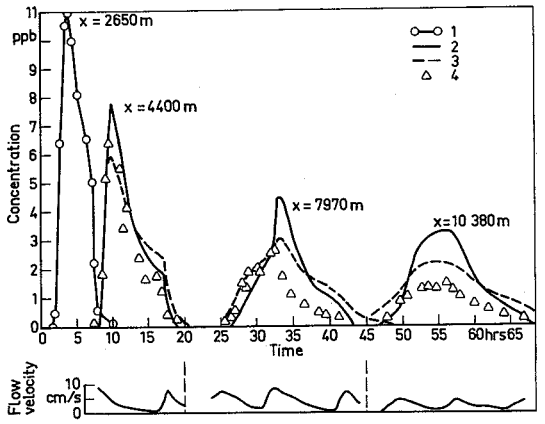

Fig. 6. Measured and simulated concentration distribution curves in the Nurmonjoki River at different locations along the river. The corresponding computed flow velocity is also shown.

Legend:
1 = measured initial concentration distribution
2 = computed concentration distribution, a = 10.
3 = computed concentration distribution, a = 25.
4 = measured concentration values

ones, as it is mass conserving. The arrival time of the peak concentration is quite accurately simulated, but the tail of the time curve not quite so accurate.

From the above experiment it is obvious that it can be difficult to deal with mixing in rivers with unsteady flow. It is therefore important to eliminate errors inherent in the calculation method. It should be clear that, if the mixing calculated by a model is mainly due to numerical diffusion, the concept of a mixing coefficient K has no relevance, it is only a best-fit parameter for this particular case. The Holly-Preissmann method, however, seems to be quite efficient in dealing with the transport and the mixing in unsteady conditions.

SUMMARY

The two mathematical models, USTFLO and DISPER, described in this article have been developed at the Hydrological Office of the National Board of Waters, Finland. The USTFLO model simulates the unsteady flow in a river, and it is especially designed to simulate the propagation of flood waves through reservoirs and along rivers and the discharge released from hydro-power plants. The USTFLO model is one-dimensional, and it solves the full de Saint Venant equations, using an implicit Preissmann-type scheme. It computes water levels and discharges in each gridpoint for each time level. It can also be applied to a tree-like branching river system. Effort has been made to make the model flexible, so that it would be easy to run the model with different boundary conditions. The USTFLO model was applied to the Nurmonjoki River, and the measured and computed water levels agreed quite well with each other.

The DISPER model simulates the convection, dispersion and decay of a tracer or a pollutant in a river with unsteady flow. It uses the flow field and water levels computed with the USTFLO model as input data. The DISPER model uses the Holly-Preissmann method of characteristics to compute the convection, and explicit difference schemes for the dispersion and decay parts of the calculation. The DISPER model was used to simulate the transport of a tracer (Rhodamine) in the Nurmonjoki River during a field experiment. It was found that significant numerical diffusion occurred when the original grid (mean $\Delta x = 564$ m) was used. After the grid was refined (mean $\Delta x = 103$ m) numerical diffusion was still present, but had decreased to an acceptable level. The propagation time of the peak concentration was correctly simulated, but the peak concentration values and the concentration distribution curves were simulated less accurately. This was mainly due to the adsorption of tracer on vegetation and bottom gravel, which could not be simulated with the model. However, the Holly-Preissmann method of calculating the pure convection was found to be appropriate.

As a general conclusion of the experience gained with the two models it can be stated that both models perform well also in highly unsteady flow situations. This is due to the favourable numerical properties of the difference schemes used in these models.

LOPPUTIIVISTELMÄ

Tässä artikkelissa esitetyt kaksi matemaattista mallia, USTFLO ja DISPER, on kehitetty vesihallituksen hydrologian toimistossa. USTFLO-mallilla simuloidaan muuttuvaa virtausta joessa. Se soveltuu erityisesti tulva-aallon etenemisen laskemiseen

jokivesistössä altaineen sekä vesivoimalaitosten virtaamapäästöjen simuloimiseen.

USTFLO-malli on yksidimensioinen. Se ratkaisee täydelliset de Saint Venant'in yhtälöt käyttäen Preissmann-tyyppistä implisiittistä kaaviota. Malli laskee vedenkorkeuden ja virtaaman kussakin hilapisteessä, ja sitä voidaan soveltaa myös haaraantuvaan jokivesistöön. Malli on pyritty tekemään joustavaksi, joten mallin käyttö eri reunaehdoilla on helppoa. USTFLO-malli sovellettiin Nurmonjokeen, ja todettiin, että havaitut ja lasketut vedenkorkeusarvot vastasivat varsin hyvin toisiaan.

DISPER-malli simuloi merkkiaineen tai jäteveden kulkeutumista, sekoittumista ja hajoamista joessa, jossa on muuttuva virtaus. Lähtötietoina DISPER käyttää USTFLO-mallilla laskettuja vedenkorkeus- ja virtaamatietoja. Mallissa kuljetusosa ratkaistaan eksplisiittisesti Holly-Preissmannin karakteristika-menetelmällä, ja sekoittumis- ja hajoamisosa ratkaistaan eksplisiittisesti tavallista finite difference-menetelmää käyttäen. DISPER-mallia käytettiin merkkiaineen (Rhodamiinin) kulkeutumisen ja sekoittumisen simulointiin Nurmonjoessa. Todettiin, että laskentaa haittasi suuri numeerinen diffuusio, kun käytettiin alkuperäistä hilapisteistöä (Δx = 564 m keskimäärin). Kun hilapisteistöä tihennettiin (Δx = 103 m keskimäärin) numeerinen diffuusio väheni kohtuulliseksi. Malli simuloi oikein merkkiaineen konsentraatiohuipun etenemisnopeuden, mutta konsentraatiohuipun arvon ja konsentraatiojakauman simulointi ei ollut aivan tarkkaa. Tämä johtui lähinnä merkkiaineen adsorptoitumisesta kasvillisuuteen ja pohjakiviin, mitä ei voitu ottaa laskennassa huomioon. Holly-Preissmann-menetelmää kulkeutumisen laskemiseksi todettiin kuitenkin oikeaksi ja tehokkaaksi.

Malleilla hankitun kokemuksen perusteella voidaan päätellä, että molemmat mallit selviytyvät hyvin myös silloin, kun virtaus muuttuu voimakkaasti. Tämä perustuu malleissa käytettyjen kaavioiden hyviin numeerisiin ominaisuuksiin.

REFERENCES

Abbott, M.B. 1979. Computational Hydraulics; Elements of the Theory of Free Surface Flows. Pitman Publishing Limited, London. 374 p.

Chow, V.T. 1959. Open Channel Hydraulics. McGraw-Hill, New York. 680 p.

Cunge, J.A., Holly Jr, F.M. & Verwey, A. 1980. Practical Aspects of Computational River Hydraulics. Pitman Publishing Limited, London. 420 p.

Forsius, J. 1984. Modeling unsteady flow in an ice-covered river. Proceedings of the fifth Northern Research Basins Symposium, Vierumäki, March 19—23, 1984. 10 p.

Forsius, J., Alasaarela, E. & Virtanen, M. 1983. Application of two transport models to a regulated river. Geophysica, Vol. 20, No. 1:71—80.

Henderson, F.M. 1966. Open channel flow. McMillan Company, New York. 522 p.

Hess, K.W. & White, F.M. 1975. Modeling the dispersal of a marked fluid in Narragansett Bay. Marine Technical Report No. 38, University of Rhode Island.

Holly, F.M. & Preissmann, A. 1977. Accurate calculation of transport in two dimensions. JHYD, ASCE, 103 No. HY11, November: 1259—1277.

Liggett, J.A. & Cunge, J.A. 1975. Numerical methods of solution of the unsteady flow equations. Chapter 4 of Unsteady Flow in Open Channels, Water Resources Publications, Fort Collins: 89—182.

Liu, H. 1977. Predicting Dispersion Coefficient of Streams. JEED, ASCE, Proc. Paper 12724, February: 59—69.

Appendix 1. Flowchart of the USTFLO model.

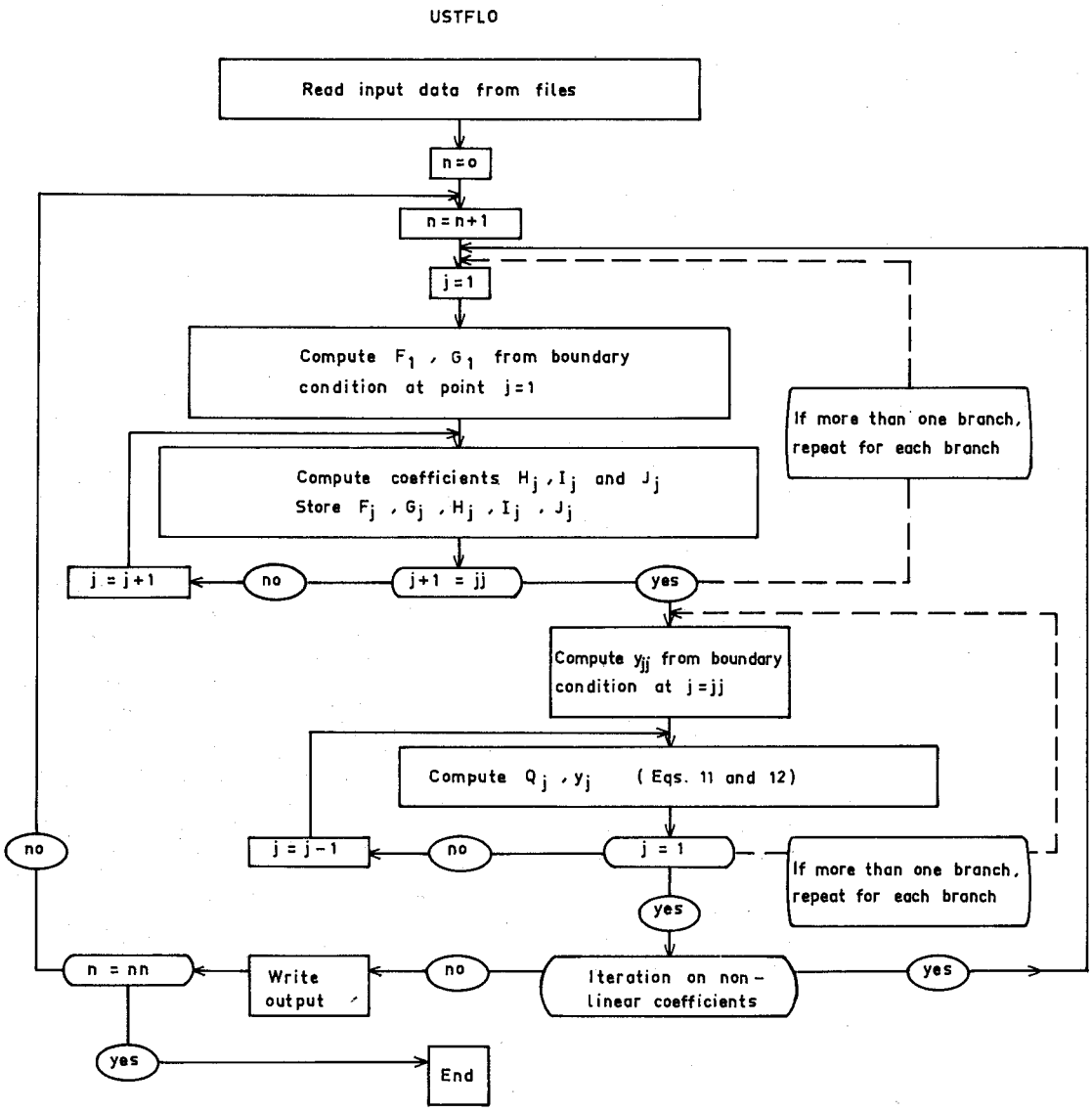

Appendix 2. Coefficients of the Preissmann-type scheme used in the USTFLO model.

$$A1_j = -\Theta$$

$$B1_j = \frac{1}{2}(b_{st})^{n+\Theta}_{j+1/2}\frac{\Delta x}{\Delta t}$$

$$C1_j = \Theta$$

$$D1_j = B1_j$$

$$E1_j = -(1-\Theta)(Q^n_{j+1} - Q^n_j) + B1_j(y^n_{j+1} + y^n_j) + q^{n+\Theta}_{j+1/2}\Delta x$$

$$A2_j = \frac{1}{2}\left(\frac{\Delta x}{\Delta t} + g\,\Delta x\,|Q^n_j|\,A^{n+1/2}_j/K^{n+1/2}_j\right) - \beta\frac{Q^n_j}{A^{n+1/2}_j}$$

$$B2_j = -\Theta\, g\, A^{n+\Theta}_{j+1/2}$$

$$C2_j = \frac{1}{2}\left(\frac{\Delta x}{\Delta t} + g\,\Delta x\,|Q^n_{j+1}|\,A^{n+1/2}_{j+1}/K^{n+1/2}_{j+1}\right) - \beta\frac{Q^n_{j+1}}{A^{n+1/2}_j}$$

$$D2_j = -B2_j$$

$$E2_j = \frac{1}{2}\frac{\Delta x}{\Delta t}(Q^n_{j+1} + Q^n_j) - g\,A^{n+\Theta}_{j+1/2}(1-\Theta)(y^n_{j+1} - y^n_j)$$

Appendix 3. List of input variables of the USTFLO model.

Input variables of the USTFLO model

Parameter file:

Variable	Type	Description
AICE(I)	Real array	Ice thickness (m) in branch I
BETA	Real	Velocity distribution coefficient β
CM(M)	Real array	Head loss coefficient in contraction M
DT	Real	Time step (s)
IBR(I)	Integer array	Order of computing first sweep in branches
ISTEP(I)	Integer array	Direction of first sweep in branch I (1 or -1)
ITER	Integer	Number of iterations
JF1(I)	Integer	Last point of branch I connects to first point of branch JF1
JFIRST(I)	Integer array	First gridpoint in branch I
JHL(M)	Integer array	Gridpoint with singular head loss
JLAST(I)	Integer array	Last gridpoint in branch I
JOUT(M)	Integer array	Gridpoint, from which output is required
L1(I)	Integer array	First gridpoint in branch I connects to last gridpoint in branch L1
L2(I)	Integer array	First gridpoint in branch I connects to last gridpoint in branch L2
NATBL	Integer	Number of water levels used to tabulate cross sectional data
NBRCHS	Integer	Number of branches
NJHL	Integer	Number of singular head loss points
NJOUT	Integer	Number of output points
NPRINT	Integer	Output is printed at time interval NPRINT*DT
QLAT(I)	Real array	Lateral inflow to branch I ($m^2\ s^{-1}$)
RADCOR(I)	Real array	Fraction of ice cover to be added to wetted perimeter values of branch I
REFLEV	Real	Reference level (m). Refers to internal computations
STRIC(I)	Real	Strickler or Manning number ($m^{1/3}\ s^{-1}$)
TCOMP	Real	Total simulation time (s, min or h)
THETA	Real	Weighting coefficient Θ
TSTART	Real	Run time before simulation starts (s, min or h). Ensures right initial conditions.
WIDTHCON	Real	Factor to decrease storage width when time < TSTART

River geometry file:

Variable	Type	Description
AREA(K,J)	Real array	Cross-sectional area (m^2) corresponding to HAP (K,J)
HAP(K,J)	Real array	Tabulated water level (m) in point j
PERIM(K,J)	Real array	Perimeter value (m) corresponding to HAP(K,J)
TXT2	Alphanumeric	Text
WIDTH(K,J)	Real array	Storage width (m) corresponding to HAP(K,J)
X(J)	Real array	Longitudinal co-ordinate (m)

Initial data file:

Variable	Type	Description
INIT	Integer	Initial data type
OUTH(J)	Real array	Initial water level in point j (m)
OUTQ(J)	Real array	Initial discharge in point j ($m^3\ s^{-1}$)

Boundary data file:

Variable	Type	Description
BF(K,I)	Real array	Tabulated first First boundary condition in branch I (s, min, h)
BL(K,I)	Real array	Tabulated last boundary condition in branch I (s, min, h or, in the case of a Q − y relation, water level in meters)
BVF(K,I)	Real array	Value of discharge or water level at first boundary corresponding to BF(K,I)
BVL(K,I)	Real array	Value of discharge or water level at last boundary corresponding to BL(K,I)
LBTYP(I)	Integer array	Type of last boundary condition in branch I
MFBTYP(I)	Integer array	Type of first boundary condition in branch I
NFPAIR(I)	Integer array	Number of pairs used to tabulate first boundary condition in branch I
NLPAIR(I)	Integer array	Number of pairs used to tabulate last boundary condition in branch I
TSCALE	Real	Multiplication factor to convert BF(K,I) and BL(K,I) time values to seconds
TXT4	Alphanumeric	Text

Appendix 4. Flowchart of the DISPER model.

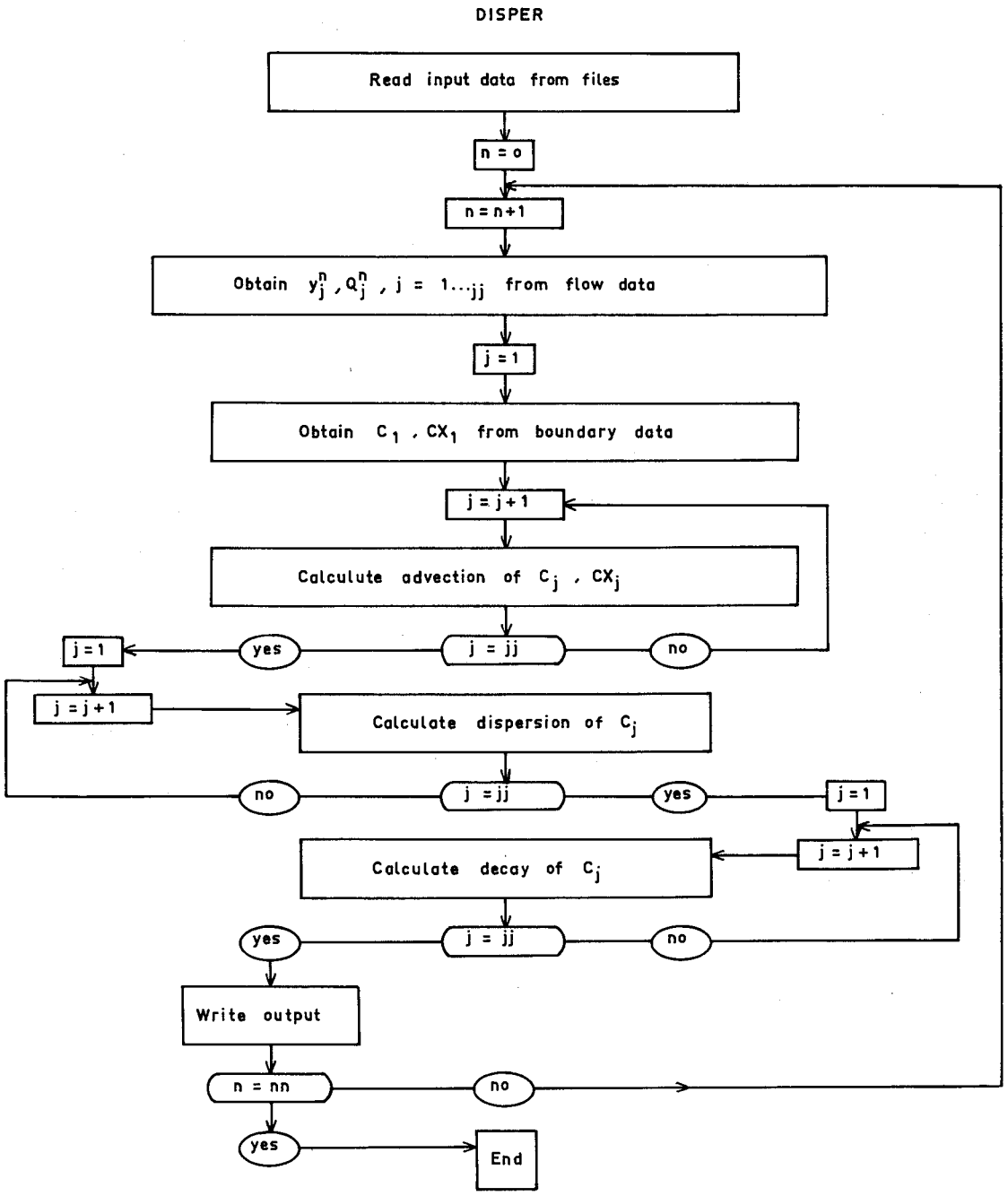

Appendix 5. List of input variables of the DISPER model.

Input variables of the DISPER model

Parameter file:

Variable	Type	Description
BEETA	Real	Mixing coefficient (Liu, 1977)
C(J)	Real array	Concentration value of point j
CX(J)	Real array	Concentration gradient value of point j
DECAY	Real	Decay coefficient (s^{-1})
DIFF	Real	Global diffusion coefficient ($m^2\ s^{-1}$)
DK	Real	Coefficient for variable diffusion (m^2)
DTADV	Real	Time step (s) for calculation of advection
DTDIFF	Real	Time step (s) for calculation of diffusion
INIT	Integer	Type of initial condition
JFIRST	Integer	First gridpoint number
JLAST	Integer	Last gridpoint number
JOUT (M)	Integer array	Gridpoint from which output is required
LSKIP	Integer	Lines to be skipped in flow data file
NATBL	Integer	Number of water levels used to tabulate cross sectional data
NJOUT	Integer	Number of output points
NPRINT	Integer	Output is printed at time interval NPRINT*DTADV
TCOMP	Real	Simulation time (s, min or h)
TSCALE	Real	Multiplication factor ot convert time to units of seconds
TSTART	Real	Difference between flow simulation time and concentration observation time (s, min or h)
TXT	Alphanumeric	Text

River geometry file:

Variable	Type	Description
AREA(K,J)	Real array	see appendix 3
HAP(K,J)	Real array	see appendix 3
PERIM(K,J)	Real array	see appendix 3
WIDTH(K,J)	Real array	see appendix 3
X(J)	Real array	see appendix 3
TXT2	Alphanumeric	Text

Flow data file:

Variable	Type	Description
HN(J)	Real array	Water level in point j
QN(J)	Real array	Discharge in point j
TN	Real	Time level

Boundary data file:

Variable	Type	Description
CB(K)	Real array	Concentration at time level TIMC (K)
CXB(K)	Real array	Concentration gradient at time level TIMC (K)
TIMC(K)	Real array	Time level
NFPAIR	Integer	Number of pairs used to tabulate boundary condition